

The curvature of the critical surface $(m_{u,d}, m_s)^{\text{crit}}(\mu)$: a progress report

Philippe de Forcrand*

*Institute for Theoretical Physics, ETH Zurich, CH-8093 Zurich, Switzerland
and
CERN, Physics Department, TH Unit, CH-1211 Geneva 23, Switzerland
E-mail: forcrand@phys.ethz.ch*

Owe Philipsen

*Institut für Theoretische Physik, Westfälische Wilhelms-Universität Münster, Germany
E-mail: ophil@uni-muenster.de*

At zero chemical potential μ , the order of the temperature-driven quark-hadron transition depends on the quark masses $m_{u,d}$ and m_s . Along a critical line bounding the region of first-order chiral transitions in the $(m_{u,d}, m_s)$ plane, this transition is second order. When the chemical potential is turned on, this critical line spans a surface, whose curvature at $\mu = 0$ can be determined without any sign or overlap problem. Our past measurements on $N_t = 4$ lattices suggest that the region of quark masses for which the transition is first order *shrinks* when μ is turned on, which makes a QCD chiral critical point at small μ/T unlikely. We present results from two complementary methods, which can be combined to yield information on higher-order terms. It turns out that the $\mathcal{O}(\mu^4)$ term reinforces the effect of the leading $\mathcal{O}(\mu^2)$ term, and there is strong evidence that the $\mathcal{O}(\mu^6)$ and $\mathcal{O}(\mu^8)$ terms do as well. We also report on simulations underway, where the strange quark is given its physical mass, and where the lattice spacing is reduced.

*The XXVI International Symposium on Lattice Field Theory
July 14 - 19, 2008
Williamsburg, Virginia, USA*

*Speaker.

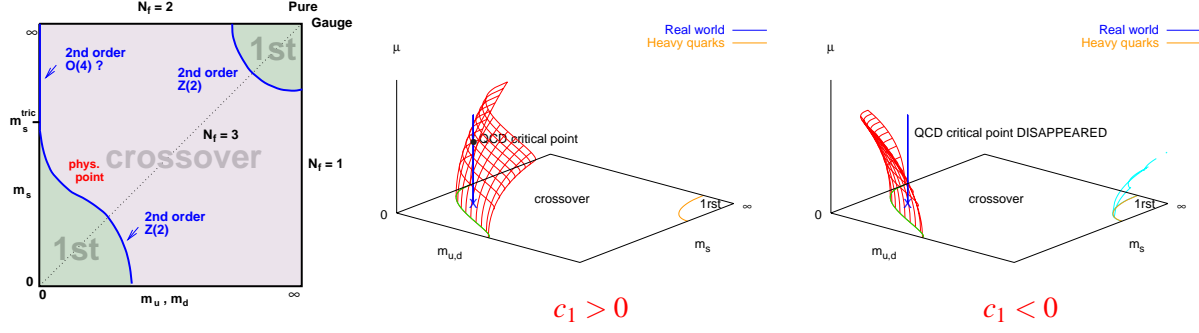


Figure 1: (Left) Schematic phase transition behavior of $N_f = 2 + 1$ QCD for different choices of quark masses ($m_{u,d}, m_s$) at $\mu = 0$. (Middle, Right) Critical surface swept by the chiral critical line as μ is turned on. Depending on the sign of the curvature c_1 , a QCD chiral critical point is present or absent [1]. For heavy quarks the curvature has been determined [2] and the first-order region shrinks with μ .

1. Introduction

The fundamental importance of the phase diagram of QCD, as a function of temperature T and quark chemical potential μ , makes it the object of several current lattice investigations. It depends sensitively on the u, d, s quark masses. At $\mu = 0$, Fig. 1 (Left) summarizes the prevalent understanding of the order of the finite-temperature quark-hadron transition as a function of $m_u = m_d$ and m_s . The physical point lies in the crossover region, separated from the chiral, first-order region by a second-order *chiral critical line*. While the $\mu = 0$ situation is far from settled, it can in principle be resolved by manageable increases in computer resources. When $\mu \neq 0$, the complex nature of the fermion determinant makes the matter much worse. While finite- μ results, including the location of the QCD critical point, have been obtained by reweighting $\mu = 0$ data [3], assessing the reliability of these results is a challenge in itself [4]. It appears that the only information that can be obtained reliably (i.e. performing thermodynamic and continuum extrapolations) in principle, barring an algorithmic breakthrough, is the Taylor expansion of thermodynamic observables in (μ/T) about $\mu = 0$. This makes the detection of a finite- μ critical point, characterized by a singularity in the free energy, particularly difficult.

To circumvent this problem, our strategy consists of Taylor-expanding the surface swept by the chiral critical line of Fig. 1 (Left). The Taylor expansion of a generic quark mass m_c on the *chiral critical surface*, and the associated transition temperature T_c , can be written as:

$$\frac{T_c(m, \mu)}{T_c(m_0^c, 0)} = 1 + \sum_{k,l=1} \alpha_{kl} \left(\frac{m - m_0^c}{\pi T_c} \right)^k \left(\frac{\mu}{\pi T_c} \right)^{2l}, \quad (1.1)$$

$$\frac{m_c(\mu)}{m_c(0)} = 1 + \sum_{k=1} c_k \left(\frac{\mu}{\pi T_c} \right)^{2k}. \quad (1.2)$$

The sign of c_1 governs the small- μ behaviour, as illustrated Fig. 1. Our first results [1], for the $N_f = 3$ ($m_s = m_{u,d}$) theory on an $8^3 \times 4$ lattice, favored a negative value for c_1 . In [5], we presented a new numerical method to obtain the c_k 's. Here, we combine the two methods and report on our

progress towards determining c_1 and higher Taylor coefficients (i) on larger lattices; (ii) for the $N_f = 2 + 1$ theory with physical m_s ; (iii) for the $N_f = 3$ theory on a finer, $N_t = 6$, lattice.

2. Extracting the μ -dependence of the critical point

On the lattice, the Taylor expansion (1.2) is replaced by that of dimensionless observables:

$$\beta_c(am, a\mu) = \beta_c(am_0^c, 0) + \sum_{k,l=1} c_{kl} (am - am_0^c)^k (a\mu)^{2l}, \quad (2.1)$$

$$am^c(a\mu) = am_0^c + \sum_{k=1} c'_k (a\mu)^{2k}. \quad (2.2)$$

To differentiate between crossover, second- and first-order transitions, we monitor the Binder cumulant of the quark condensate:

$$B_4 \equiv \frac{\langle(\delta\bar{\psi}\psi)^4\rangle}{\langle(\delta\bar{\psi}\psi)^2\rangle^2}, \quad \delta\bar{\psi}\psi = \bar{\psi}\psi - \langle\bar{\psi}\psi\rangle, \quad (2.3)$$

when $\langle(\delta\bar{\psi}\psi)^3\rangle = 0$. On the chiral critical surface, B_4 takes value 1.604 as dictated by the 3d Ising universality class. It can be expanded as:

$$B_4(am, a\mu) = 1.604 + \sum_{k,l=1} b_{kl} (am - am_0^c)^k (a\mu)^{2l}, \quad (2.4)$$

with coefficients satisfying the scaling behaviour $b_{kl}(L) = f_{kl}L^{(k+l)/\nu}$ for large L . Having measured the first few b_{kl} 's by the methods of Sec. 3, we can reconstruct the c'_k 's eq.(2.2) as:

$$c'_1 = \frac{dam^c}{d(a\mu)^2} = -\frac{\partial B_4}{\partial(a\mu)^2} \left(\frac{\partial B_4}{\partial am} \right)^{-1} = -\frac{b_{01}}{b_{10}}, \quad (2.5)$$

$$c'_2 = \frac{1}{2!} \frac{d^2 am^c}{d[(a\mu)^2]^2} = -\frac{1}{b_{10}} (b_{02} + b_{11}c'_1 + b_{20}c_1'^2). \quad (2.6)$$

and finally c_1 and c_2 as:

$$c_1 = \frac{\pi^2}{N_t^2} \frac{c'_1}{am_0^c} + \frac{1}{T_c(m_0^c, 0)} \frac{dT_c(m^c(\mu), \mu)}{d(\mu/\pi T)^2}, \quad (2.7)$$

$$c_2 = \frac{\pi^4}{N_t^4} \frac{c'_2}{am_0^c} - \frac{\pi^2}{N_t^2} \frac{c'_1}{am_0^c} \frac{1}{T_c(m_0^c, 0)} \frac{dT_c(m^c(\mu), \mu)}{d(\mu/\pi T)^2} + \frac{1}{2T_c(m_0^c, 0)} \frac{d^2 T_c(m^c(\mu), \mu)}{d[(\mu/\pi T)^2]^2}. \quad (2.8)$$

3. Two methods to measure B_4 derivatives

B_4 varies steeply with the quark mass, and b_{10}, b_{20} in eq.(2.4) can be obtained straightforwardly from fits of B_4 measured at $\mu = 0$ for different quark masses [1]. Measuring the variation of B_4 with μ is another matter: B_4 is a noisy quantity, its variation is small, and simulating at non-zero (real) μ is not feasible. We have used two different, complementary methods to bypass these difficulties [5]:
1. We perform simulations at several imaginary values $\mu = i\mu_i$, where the sign problem is absent, and fit our measurements of $B_4(\mu_i)$ with a truncated Taylor series in μ^2 .

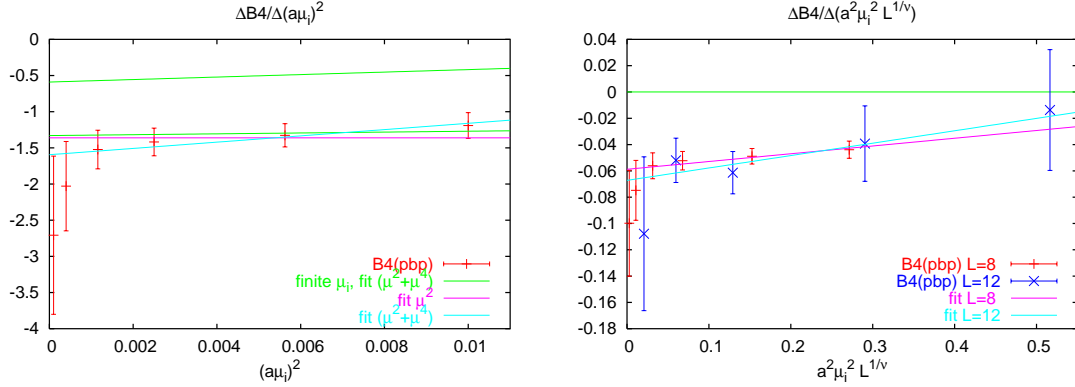


Figure 2: (*Left*) Comparison of two methods of measuring $\partial B_4 / \partial (a\mu_i)^2$ on an $8^3 \times 4$ lattice. The broad error band is the fit to imaginary μ data; the data points show the reweighted finite difference quotients, obtained with about 4 times fewer statistics. (*Right*) Finite-size scaling test: data obtained on 8^3 and $12^3 \times 4$ lattices show good consistency with the $3d$ Ising universality class.

2. We perform simulations at $\mu = 0$, reweight to small values $\mu = i\mu_i$, and measure the finite difference quotients $\Delta B_4 / \Delta (a\mu)^2$, with

$$\lim_{\Delta(a\mu^2) \rightarrow 0} \frac{\Delta B_4}{\Delta (a\mu)^2} = \left. \frac{\partial B_4}{\partial (a\mu)^2} \right|_{\mu=0}. \quad (3.1)$$

A comparison between the two methods is provided Fig. 2 (*Left*), on an $8^3 \times 4$ lattice for $N_f = 3$. The error band is the fit to the finite- μ_i data (method 1). The data points are the finite-difference quotients (method 2). Consistency between the two methods is observed. The second method is clearly more efficient, since the statistics is only 1/4 of the other. This efficiency can be traced to the strong cancellation of statistical fluctuations when measuring ΔB_4 on the $\mu = 0$ and the reweighted ensemble. Reweighting itself is done stochastically with a Gaussian-distributed vector η , since the reweighting factor is

$$\rho(\mu_1, \mu_2) = \frac{\det^{N_f/4} \mathcal{D}(U, \mu_2)}{\det^{N_f/4} \mathcal{D}(U, \mu_1)} = \left\langle \exp \left(-|\mathcal{D}^{-N_f/8}(\mu_2) \mathcal{D}^{+N_f/8}(\mu_1) \eta|^2 + |\eta|^2 \right) \right\rangle_{\eta}. \quad (3.2)$$

Note the small values of $(a\mu_i)^2$ in Fig. 2 (*Left*): they guarantee a good overlap between the $\mu = 0$ Monte Carlo ensemble and the reweighted $\mu = i\mu_i$ ensemble, and small fluctuations in ρ .

Since our 8^3 lattice is not very large ($m_\pi L \sim 3.4$), we performed a finite-size scaling check by comparing with a $12^3 \times 4$ lattice. Fig. 2 (*Right*) shows nice consistency with the expected large volume universal behaviour, not only for the y-axis intercept yielding b_{01} , but also for the slope yielding b_{02} . The result ($b_{02} > 0$ like b_{01}) reinforces the finding that the transition weakens and turns into a crossover (i.e. B_4 increases) as μ is turned on (see eq. (2.4)).

Finally, we can combine the data from our two methods, since the simulations were performed independently and cover different ranges of μ_i . A combined fit of the $am = 0.0265$ data Fig. 3 shows that $(B_4(a\mu_i) - B_4(\mu = 0)) / (a\mu_i)^2$ is an alternating series in $(a\mu_i)^2$ [7]. The fit gives

$$B_4(a\mu_i) = B_4(\mu = 0) - 1.79(14)(a\mu_i)^2 + 108(27)(a\mu_i)^4 - 3438(933)(a\mu_i)^6 + 35954(8876)(a\mu_i)^8 \quad (3.3)$$

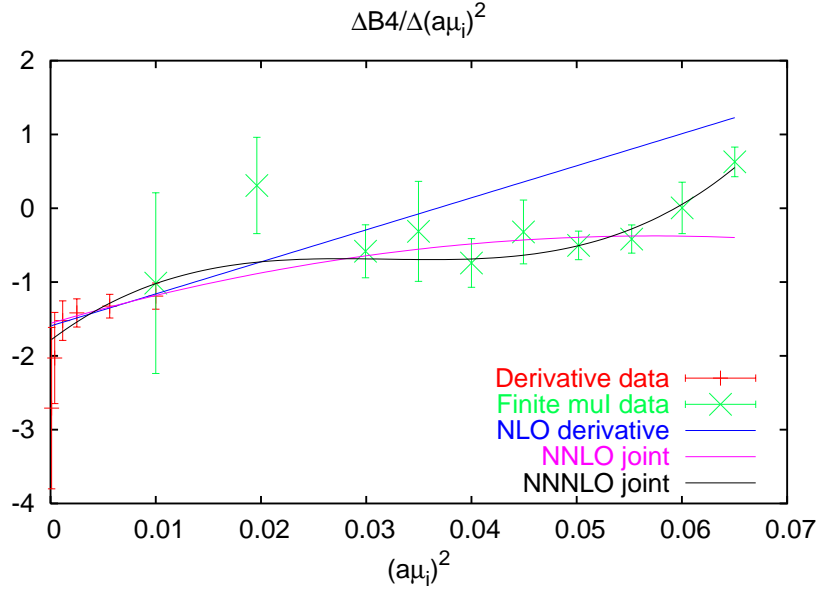


Figure 3: Combining the two methods: the $(a\mu_i)^2 \leq 0.01$ data come from $\mu = 0$ reweighting, the $(a\mu_i)^2 \geq 0.01$ from direct $\mu_i \neq 0$ simulations, all at $am = 0.0265$. Data at larger μ_i clearly fall below the $\mathcal{O}(\mu_i^4)$ contribution, indicating a negative μ_i^6 -term. The quality of the cubic, S-shape fit favors a positive μ_i^8 -term. After rotation to real μ , all terms contribute to increasing B_4 , i.e. pushing the system in the crossover region.

with a $\chi^2/\text{d.o.f.}$ of 0.57. The large values of higher-order coefficients indicate that higher-order terms become important when $\mu/T \gtrsim 0.5$. However, after rotation to real μ , they all tend to *increase* B_4 , pushing the system deeper in the crossover region. This only increases the validity of the exotic scenario Fig. 1 (*Right*) up to larger values of μ/T . Conservatively, we trust only the $\mathcal{O}(\mu^2)$ and $\mathcal{O}(\mu^4)$ terms. After continuum conversion following eqs.(2.5-2.8), our final result for $N_f = 3$ on coarse, $N_t = 4$, lattices reads [6]:

$$\frac{m_c(\mu)}{m_c(0)} = 1 - 3.3(3) \left(\frac{\mu}{\pi T}\right)^2 - 47(20) \left(\frac{\mu}{\pi T}\right)^4 - \dots \quad (3.4)$$

4. Towards the $N_f = 2 + 1$ continuum limit

We are currently investigating two reasons why our result eq.(3.4) could change qualitatively as we consider real QCD. The sign of the curvature could change as we move along the critical line away from the degenerate $N_f = 3$ case. It could also change as we take the continuum limit.

The first possibility appears unlikely given our current results Fig. 4 (*Left*), where m_s is given its physical value on the $N_t = 4$ critical line determined in [1] (see Fig. 4 (*Right*)). Since our pions are lighter than in nature, large lattices are required and thereby large computer resources. This is achieved, like for the $N_f = 3, 8^3 \times 4$, method **2** case above, by dispatching our simulations over the computing Grid. Many independent Monte Carlo runs are performed, all at $\mu = 0$, over a range of temperatures near T_c , using prioritized scheduling. Current statistics reach 600k thermalized configurations.

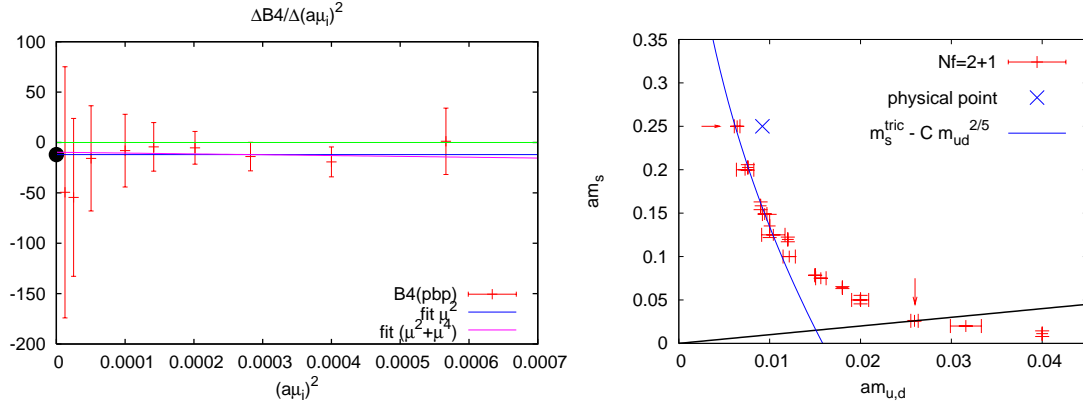


Figure 4: Work in progress: (Left) $N_f = 2 + 1$ on a $16^3 \times 4$ lattice. The simulation point, indicated by the leftmost arrow (Right), lies to the left of the physical point, implying that our pions are lighter than in nature.

The effect of a finer lattice is studied by simulating $18^3 \times 6$ lattices with $N_f = 3$ degenerate flavors. The current results, Fig. 5 (Left), give opposite signs for b_{01} using a leading or subleading order fit. While the sign of the curvature c_1 is consequently not clear, one can already say that $|c_1|$ is not large, $\mathcal{O}(20)$ or less. Thus, the critical surface is almost vertical.

In addition, another qualitative effect takes place: the $\mu = 0$ critical line, and thereby the whole chiral critical surface, moves towards the origin as $a \rightarrow 0$. For instance, the $N_f = 3$ pion mass on the critical line drops from $1.680(4)T_c$ to $0.954(12)T_c$ going from $N_t = 4$ to $N_t = 6$ lattices [5]. The first-order region, in physical units, shrinks dramatically as $a \rightarrow 0$. To compensate this effect and maintain a critical point for real QCD at small chemical potentials $\mu/T \lesssim 1$, a large positive curvature c_1 would be needed. We presently do not see it.

Finally, we note that effective models like PNJL [8] or linear sigma model [9], with simple modifications, can reproduce the qualitative features of the chiral critical surface which we observe. Nevertheless, let us stress again that our study concerns only the *chiral* critical surface, swept by the $\mu = 0$ *chiral* critical line as the chemical potential is turned on. Our results do not preclude other phase transitions, not connected to the chiral one.

Acknowledgements:

This work is partially supported by the German BMBF, project *Hot Nuclear Matter from Heavy Ion Collisions and its Understanding from QCD*, No. 06MS254. We thank the Minnesota Supercomputer Institute for providing computer resources, and the CERN IT/GS group for their invaluable assistance and collaboration using the EGEE Grid for part of this project. We acknowledge the usage of EGEE resources (EU project under contracts EU031688 and EU222667). Computing resources have been contributed by a number of collaborating computer centers, most notably HLRS Stuttgart (GER), NIKHEF (NL), CYFRONET (PL), CSCS (CH) and CERN.

References

- [1] P. de Forcrand and O. Philipsen, JHEP **0701** (2007) 077 [hep-lat/0607017].

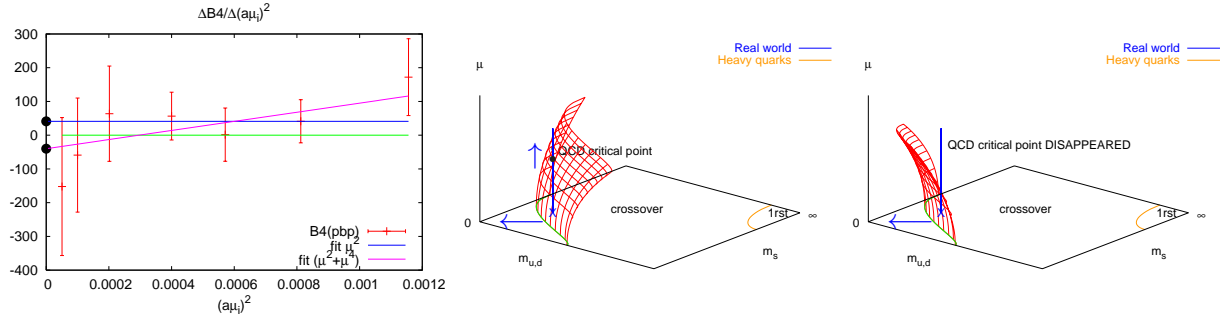


Figure 5: Work in progress: (Left) $N_f = 3$ on an $18^3 \times 6$ lattice. The sign of the intercept b_{01} depends on the fitting ansatz. (Middle) As the lattice spacing is reduced, the critical surface moves towards the origin. If a critical point exists, its location moves to larger μ . (Right) If the curvature c_1 is negative, higher-order terms must increase in magnitude for a critical point to occur.

- [2] S. Kim, Ph. de Forcrand, S. Kratochvila and T. Takaishi, PoS **LAT2005**, (2006) 166 [arXiv:hep-lat/0510069].
- [3] Z. Fodor and S. D. Katz, JHEP **0203** (2002) 014 [arXiv:hep-lat/0106002]; Z. Fodor and S. D. Katz, JHEP **0404** (2004) 050 [arXiv:hep-lat/0402006].
- [4] S. Ejiri, Phys. Rev. D **69** (2004) 094506 [arXiv:hep-lat/0401012]. K. Splittorff, arXiv:hep-lat/0505001; PoS **LAT2006** (2006) 023 [arXiv:hep-lat/0610072].
- [5] P. de Forcrand, S. Kim and O. Philipsen, PoS **LAT2007** (2007) 178 [arXiv:0711.0262 [hep-lat]].
- [6] P. de Forcrand and O. Philipsen, JHEP **0811** (2008) 012 [arXiv:0808.1096 [hep-lat]].
- [7] P. Cea, L. Cosmai, M. D'Elia and A. Papa, Phys. Rev. D **77** (2008) 051501 [arXiv:0712.3755 [hep-lat]].
- [8] K. Fukushima, arXiv:0809.3080 [hep-ph].
- [9] E. S. Bowman and J. I. Kapusta, arXiv:0810.0042 [nucl-th].